IRF1_Decoy_ChIPseq

Prepared by Zhe Zhang

August 20, 2014

Contents

1 Summary statistics **1**

1.1 Total number of mapped reads . . . 1
1.2 Strand frequency . . . 1
1.3 Base N frequency . . . 2
1.4 GC frequency . . . 2
1.5 Total mapping locations . . . 3
1.6 Duplicated mapping frequency . . . 3
1.7 Sequencing quality . . . 4
1.8 Mapping quality . . . 4
1.9 Mapping length . . . 5
1.10 Sequencing depth . . . 5
1.11 Read enrichment within promoters . . . 6
1.12 Read enrichment within 5-UTR . . . 6
1.13 Mapping with insertions . . . 7
1.14 Mapping with deletions . . . 7
1.15 K-mer frequency . . . 8

2 ChIP-seq **9**

2.1 Strand-strand correlation . . . 9
2.2 Total peaks . . . 9
2.3 5-UTR peaks . . . 12
2.4 TSS reads . . . 13

1 Summary statistics

1.1 Total number of mapped reads

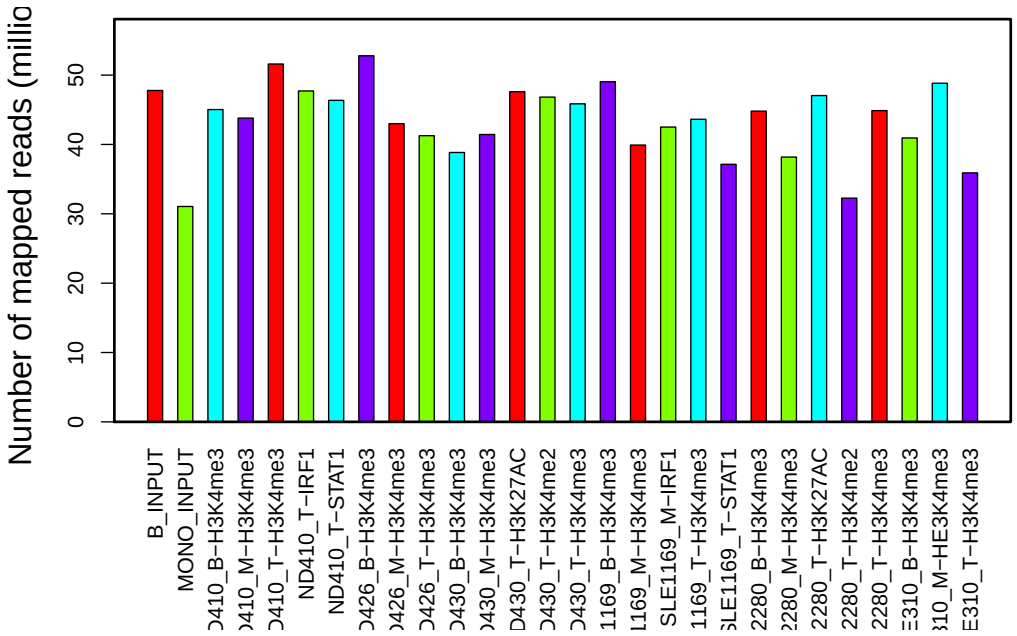

1.2 Strand frequency

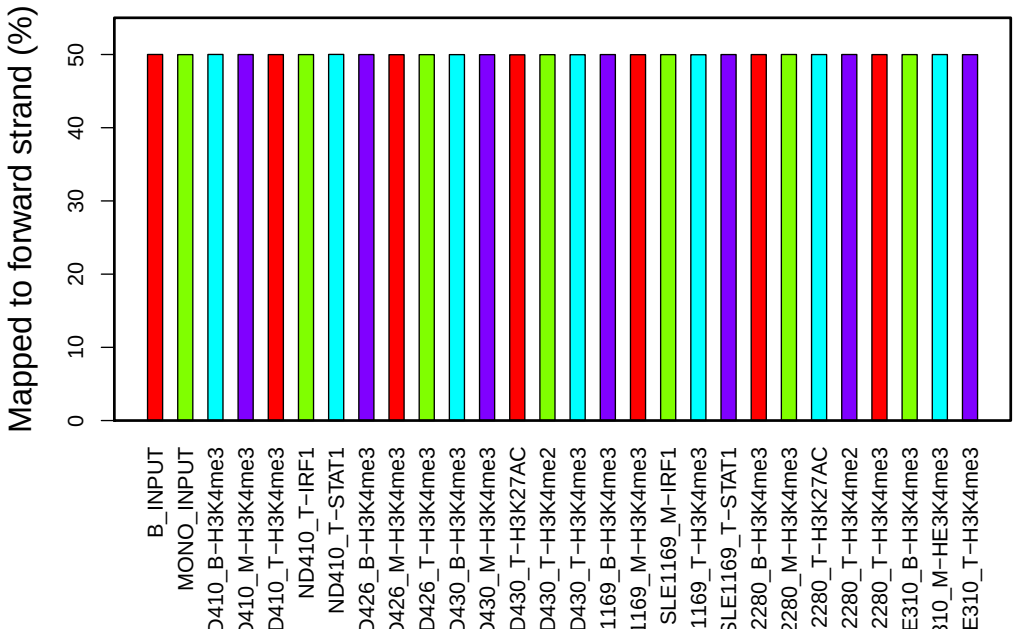

1.3 Base N frequency

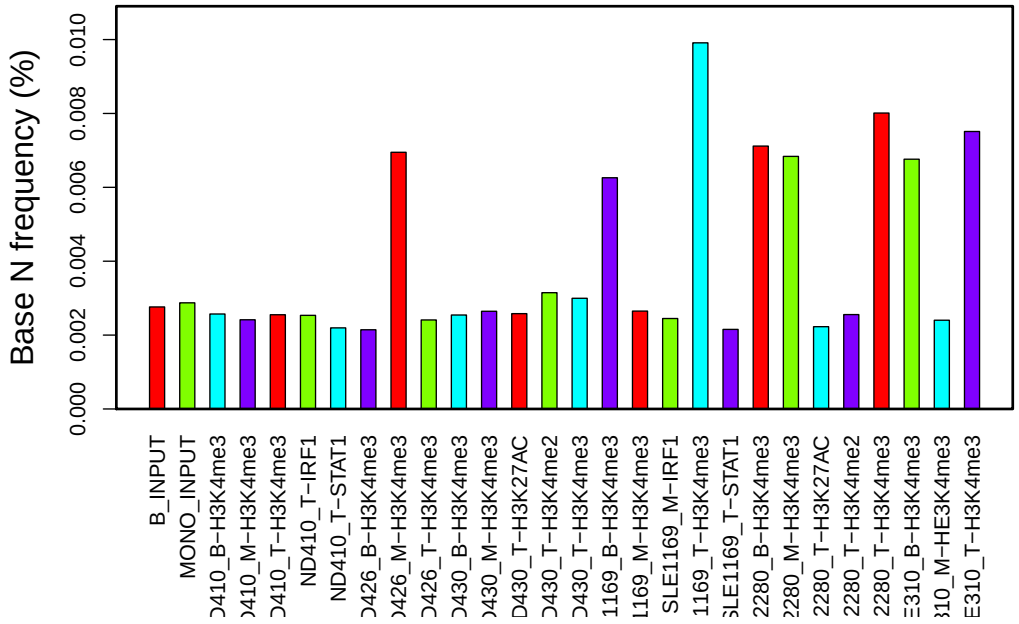

1.4 GC frequency

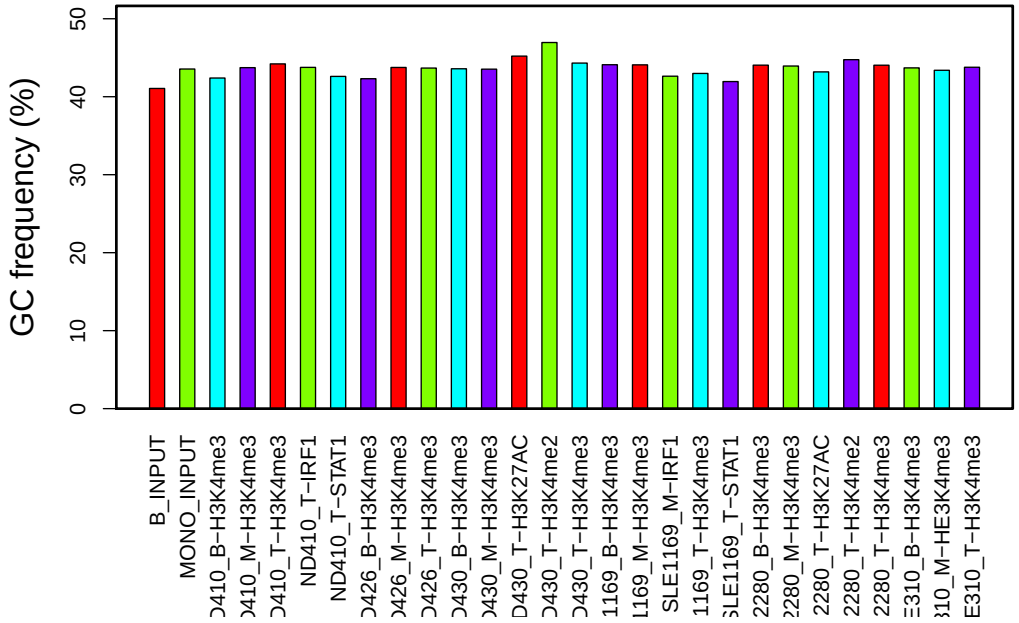

1.5 Total mapping locations

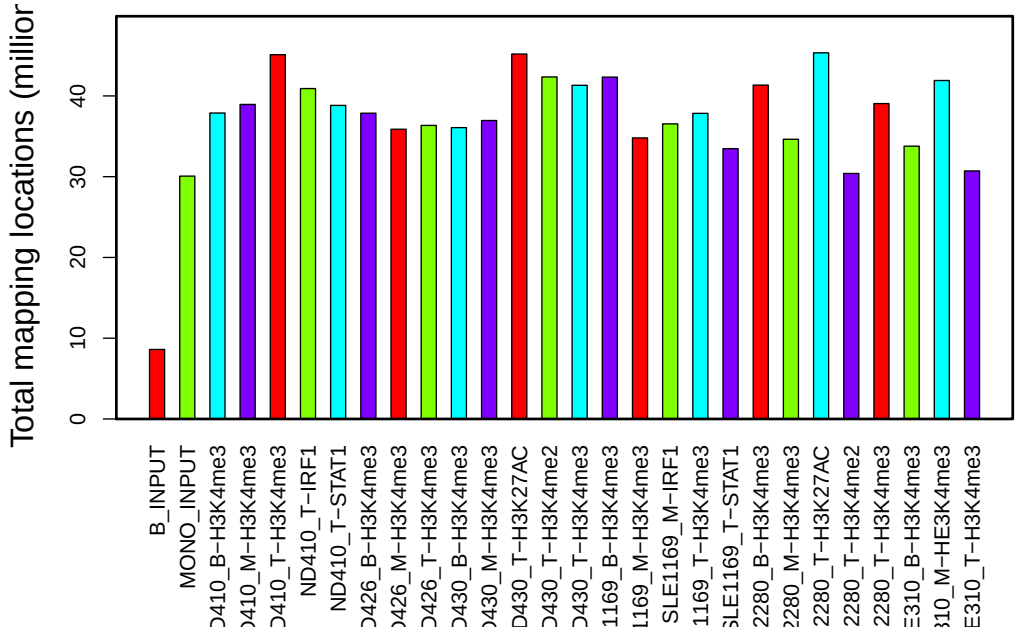

1.6 Duplicated mapping frequency

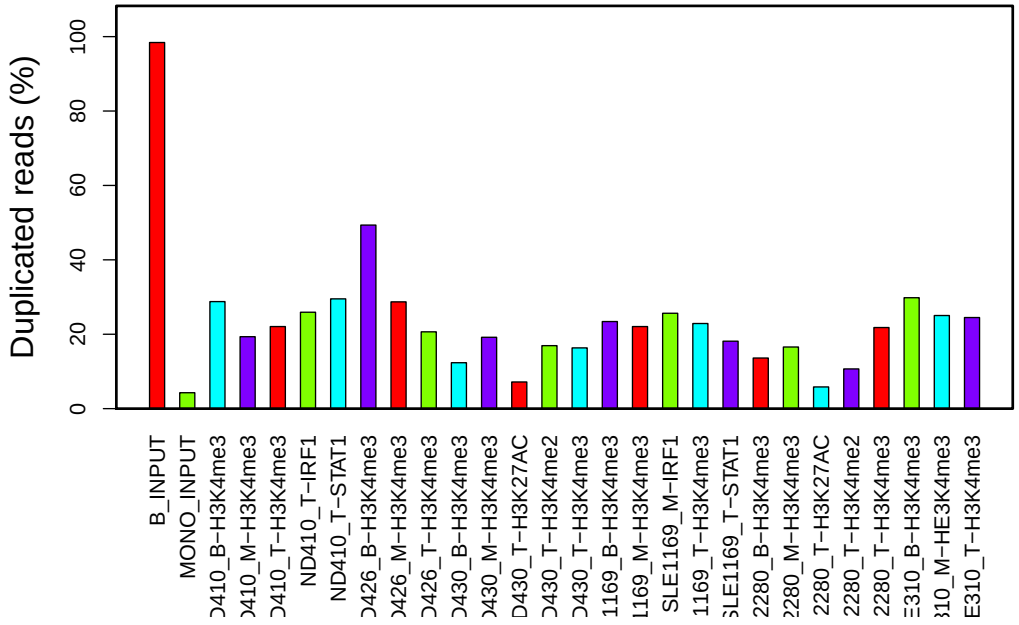

1.7 Sequencing quality

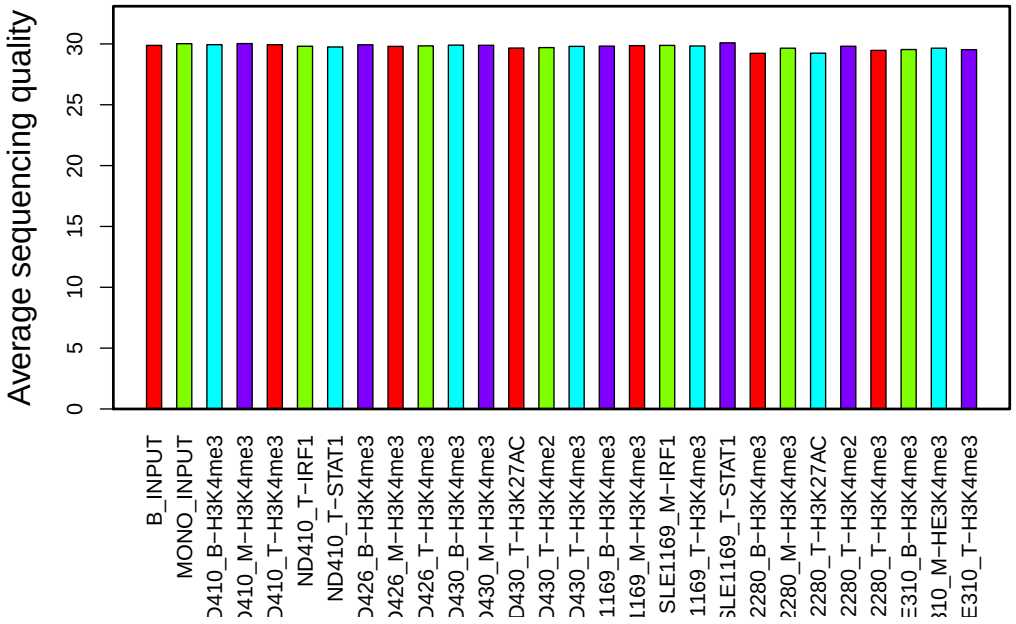

1.8 Mapping quality

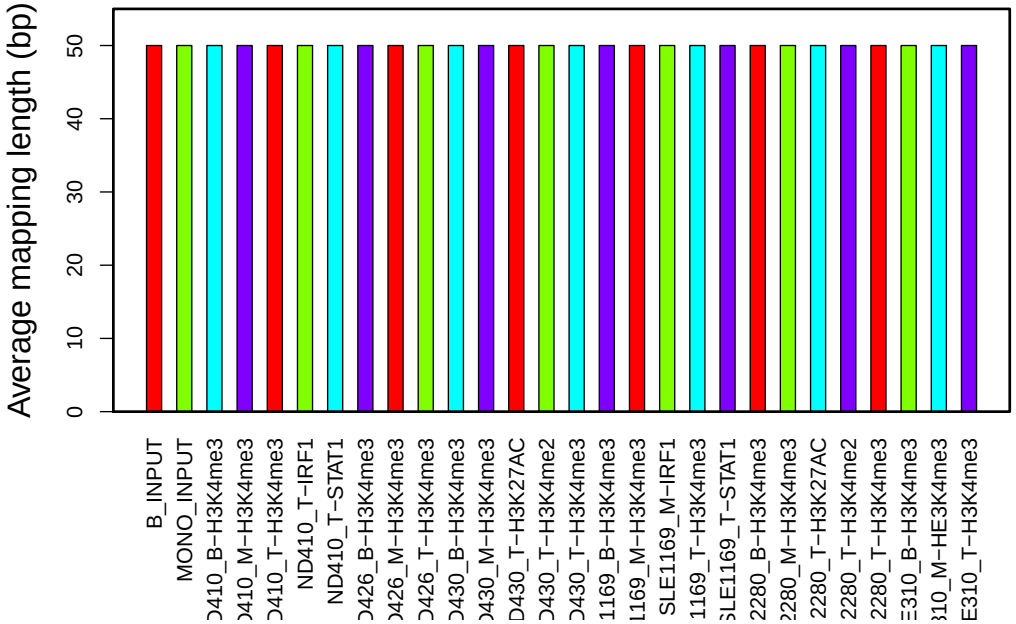

1.9 Mapping length

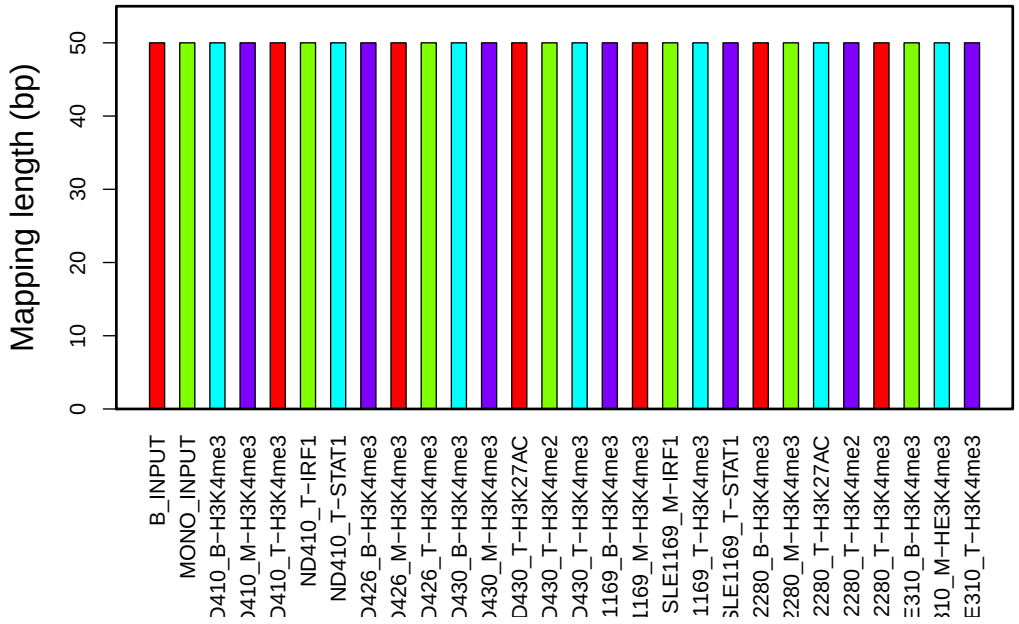

1.10 Sequencing depth

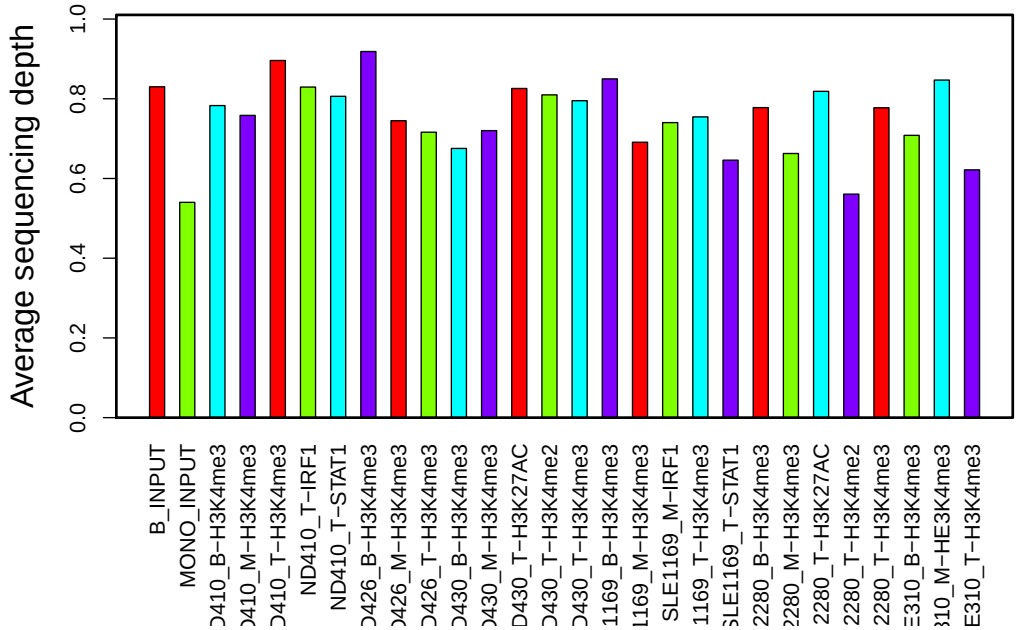

1.11 Read enrichment within promoters

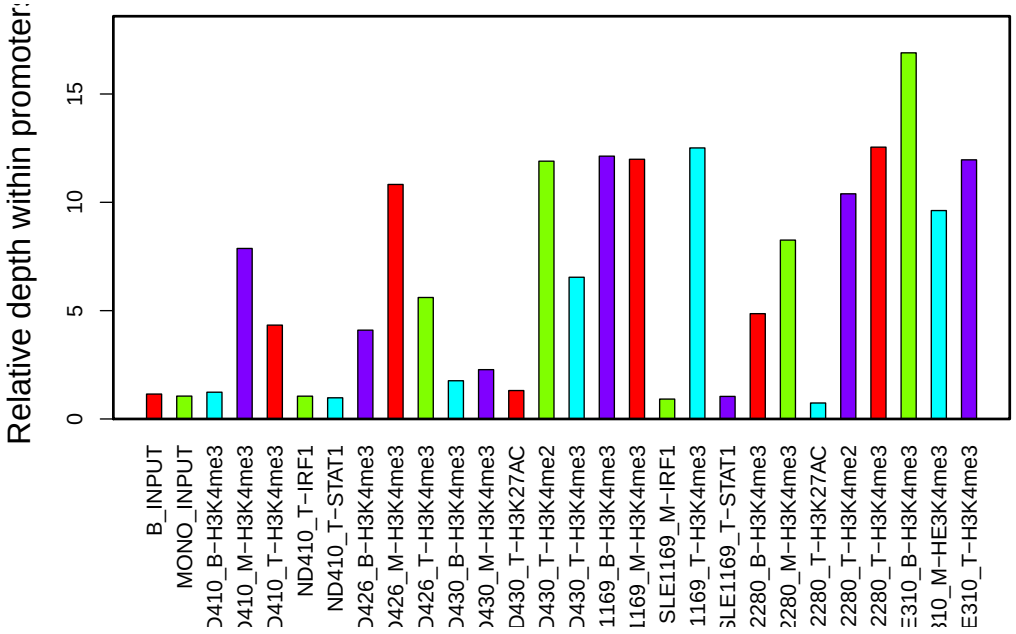

1.12 Read enrichment within 5-UTR

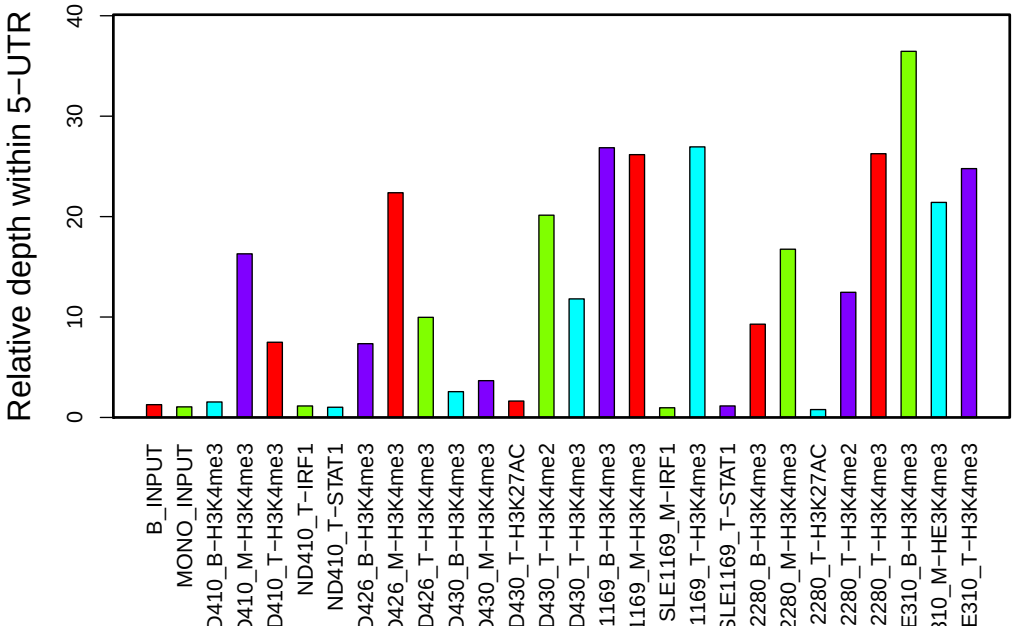

1.13 Mapping with insertions

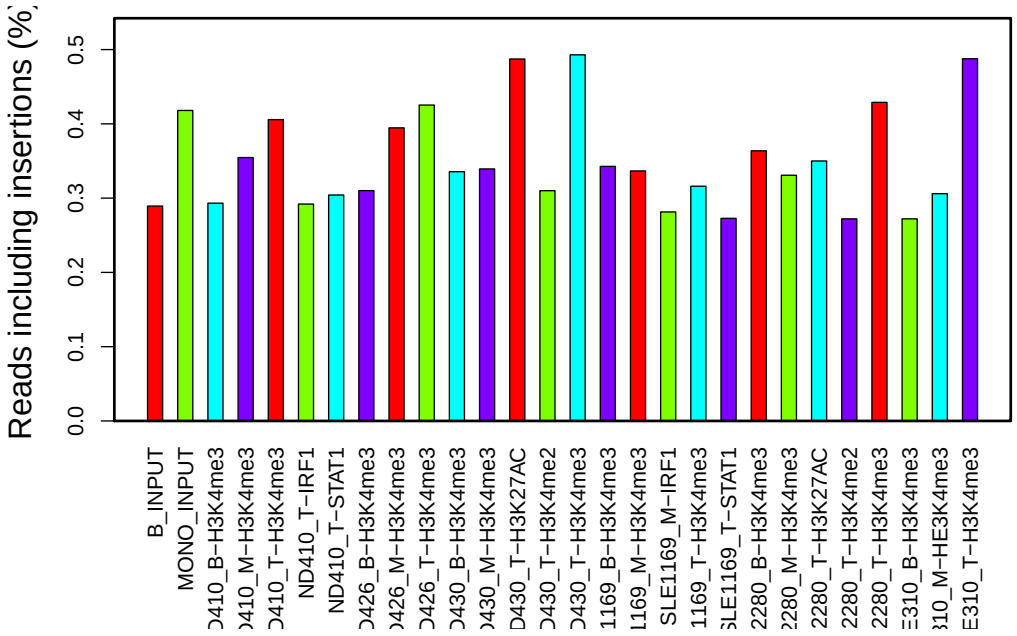

1.14 Mapping with deletions

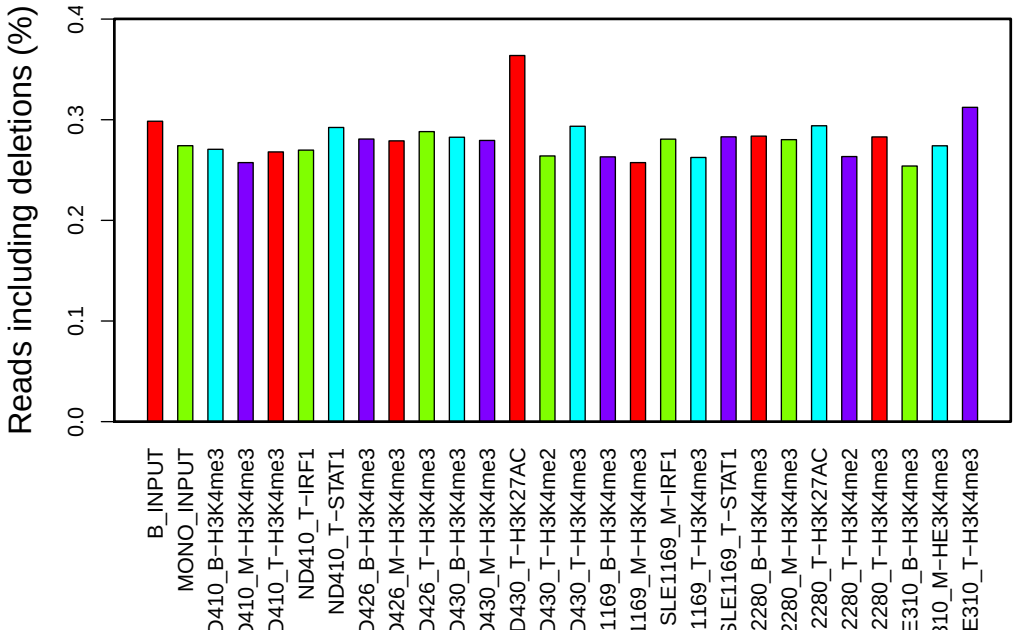

1.15 K-mer frequency

	MEAN	BINPUT	MONOINPUT	ND410B.H3K4me3	ND410M.H3K4me3	ND410T.H3K4me3	ND410T.IRF1	ND410T.STAT1	ND426B.H3K4me3	ND426M.H3K4me3	ND426T.H3K4
|CCCAG	3.55	5.05	3.54	3.31	3.67	3.45	3.46	3.63	3.25	3.10	
|CTGGG	3.52	4.43	3.21	3.60	3.66	3.34	3.83	4.08	3.68	3.34	
CCCAG|	3.51	2.97	3.17	3.47	3.59	3.23	3.53	3.55	3.65	3.30	
|CCAGG	3.37	3.51	3.24	3.04	2.94	3.58	3.47	3.06	3.49	3.24	
CTGGG|	3.24	2.51	3.21	3.51	3.26	2.99	3.42	3.56	3.22	3.47	
GGAGG|	3.23	3.12	3.29	2.82	3.19	3.18	2.76	3.17	3.05	3.07	
CCAGG|	3.12	3.61	3.01	2.96	3.49	2.74	2.98	3.06	3.05	3.27	
|CCTGG	3.11	3.60	2.91	3.32	2.82	2.95	3.33	3.38	3.14	3.69	
CCTGG|	3.03	3.61	2.92	2.83	3.03	3.04	2.78	2.97	3.21	2.88	
|GCTGG	3.03	1.61	2.67	2.83	2.90	3.21	3.35	2.60	2.89	3.20	
GGCTG|	3.00	3.32	2.66	2.89	3.06	2.96	3.03	3.10	3.25	2.94	

2 ChIP-seq

2.1 Strand-strand correlation

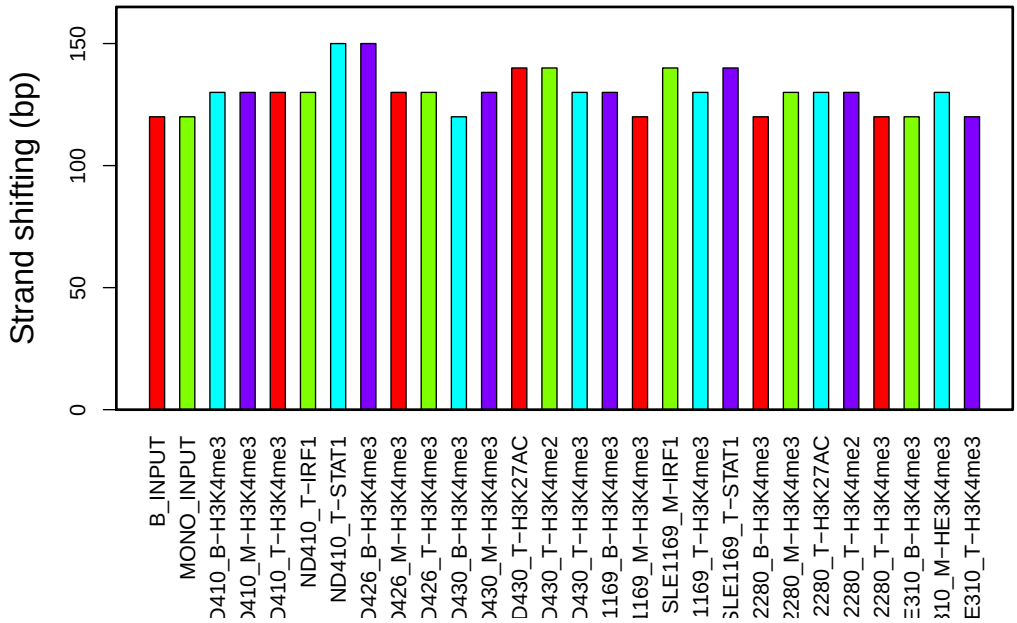

2.2 Total peaks

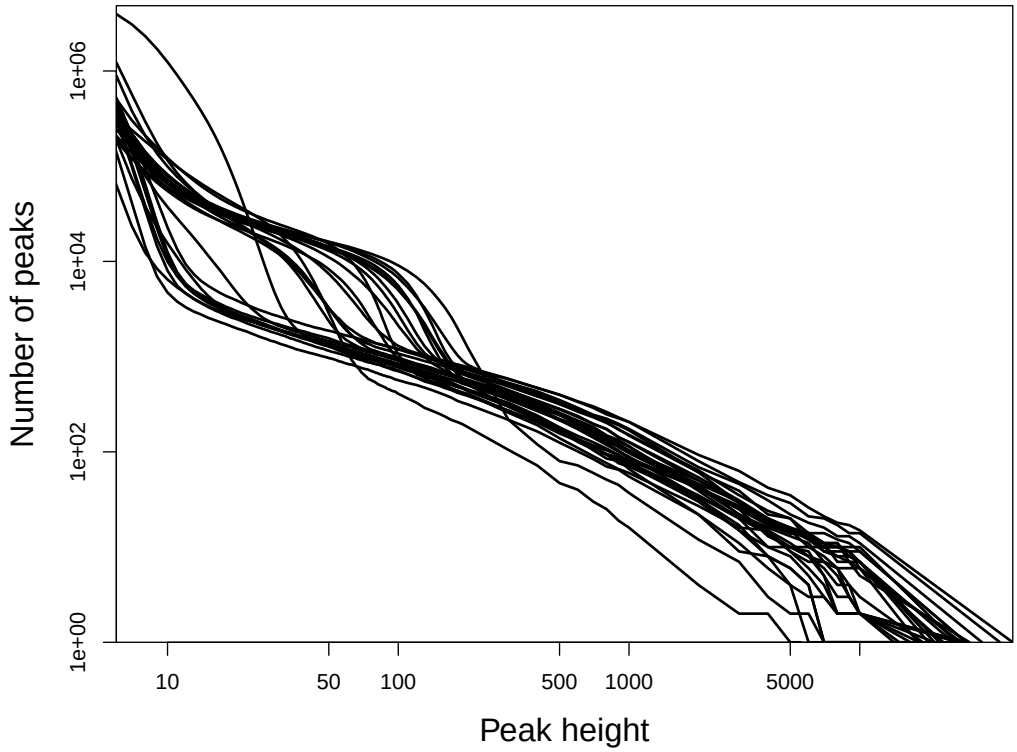

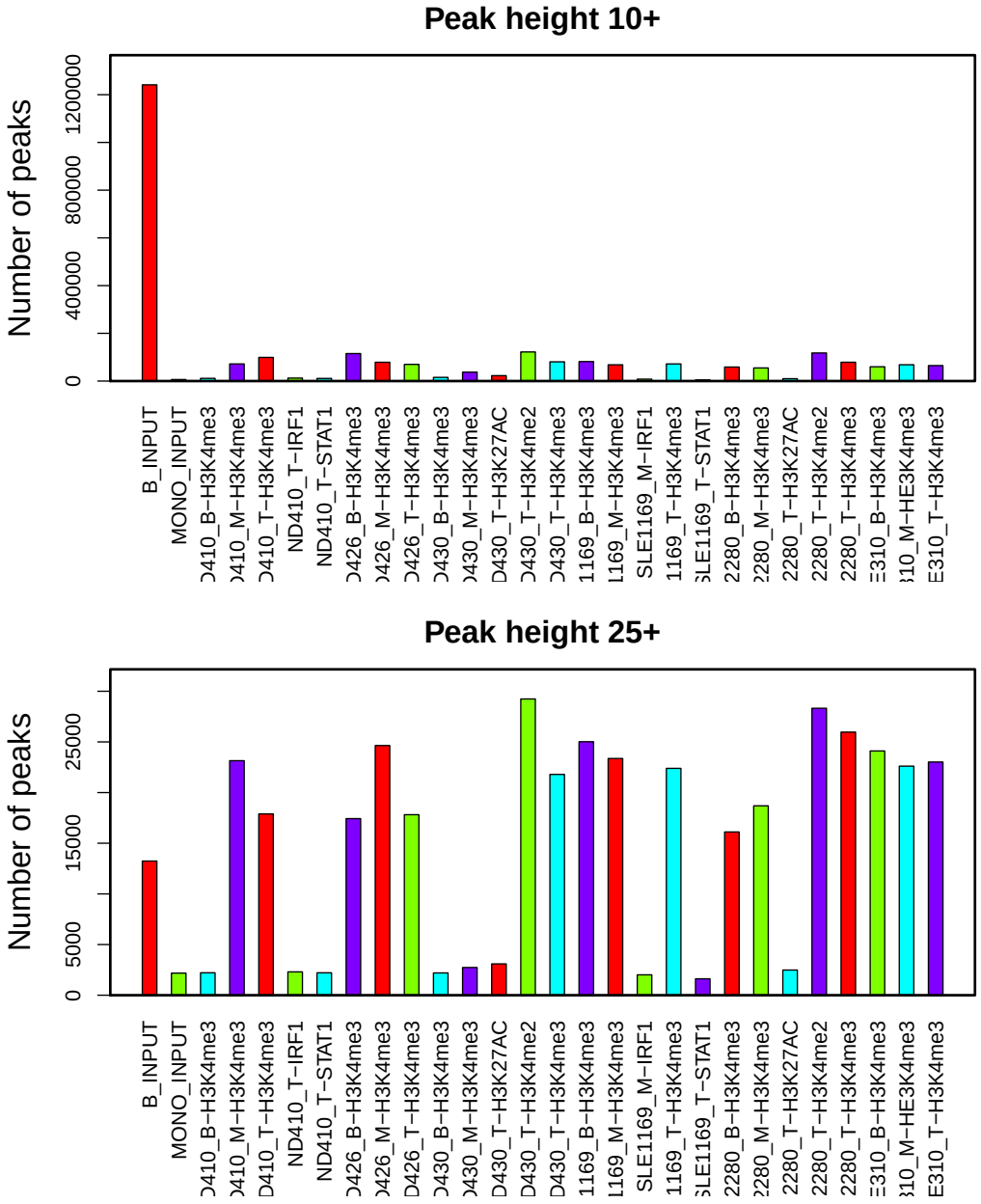
Peak height 10+
Number of peaks
0
400000
800000
1200000
B_INPUT
MONO_INPUT
D410_B−H3K4me3
D410_M−H3K4me3
D410_T−H3K4me3
ND410_T−IRF1
ND410_T−STAT1
D426_B−H3K4me3
D426_M−H3K4me3
D426_T−H3K4me3
D430_B−H3K4me3
D430_M−H3K4me3
D430_T−H3K27AC
D430_T−H3K4me2
D430_T−H3K4me3
1169_B−H3K4me3
1169_M−H3K4me3
SLE1169_M−IRF1
1169_T−H3K4me3
SLE1169_T−STAT1
2280_B−H3K4me3
2280_M−H3K4me3
2280_T−H3K27AC
2280_T−H3K4me2
2280_T−H3K4me3
E310_B−H3K4me3
310_M−HE3K4me3
E310_T−H3K4me3
Peak height 25+
Number of peaks
0
5000
15000
25000
B_INPUT
MONO_INPUT
D410_B−H3K4me3
D410_M−H3K4me3
D410_T−H3K4me3
ND410_T−IRF1
ND410_T−STAT1
D426_B−H3K4me3
D426_M−H3K4me3
D426_T−H3K4me3
D430_B−H3K4me3
D430_M−H3K4me3
D430_T−H3K27AC
D430_T−H3K4me2
D430_T−H3K4me3
1169_B−H3K4me3
1169_M−H3K4me3
SLE1169_M−IRF1
1169_T−H3K4me3
SLE1169_T−STAT1
2280_B−H3K4me3
2280_M−H3K4me3
2280_T−H3K27AC
2280_T−H3K4me2
2280_T−H3K4me3
E310_B−H3K4me3
310_M−HE3K4me3
E310_T−H3K4me3

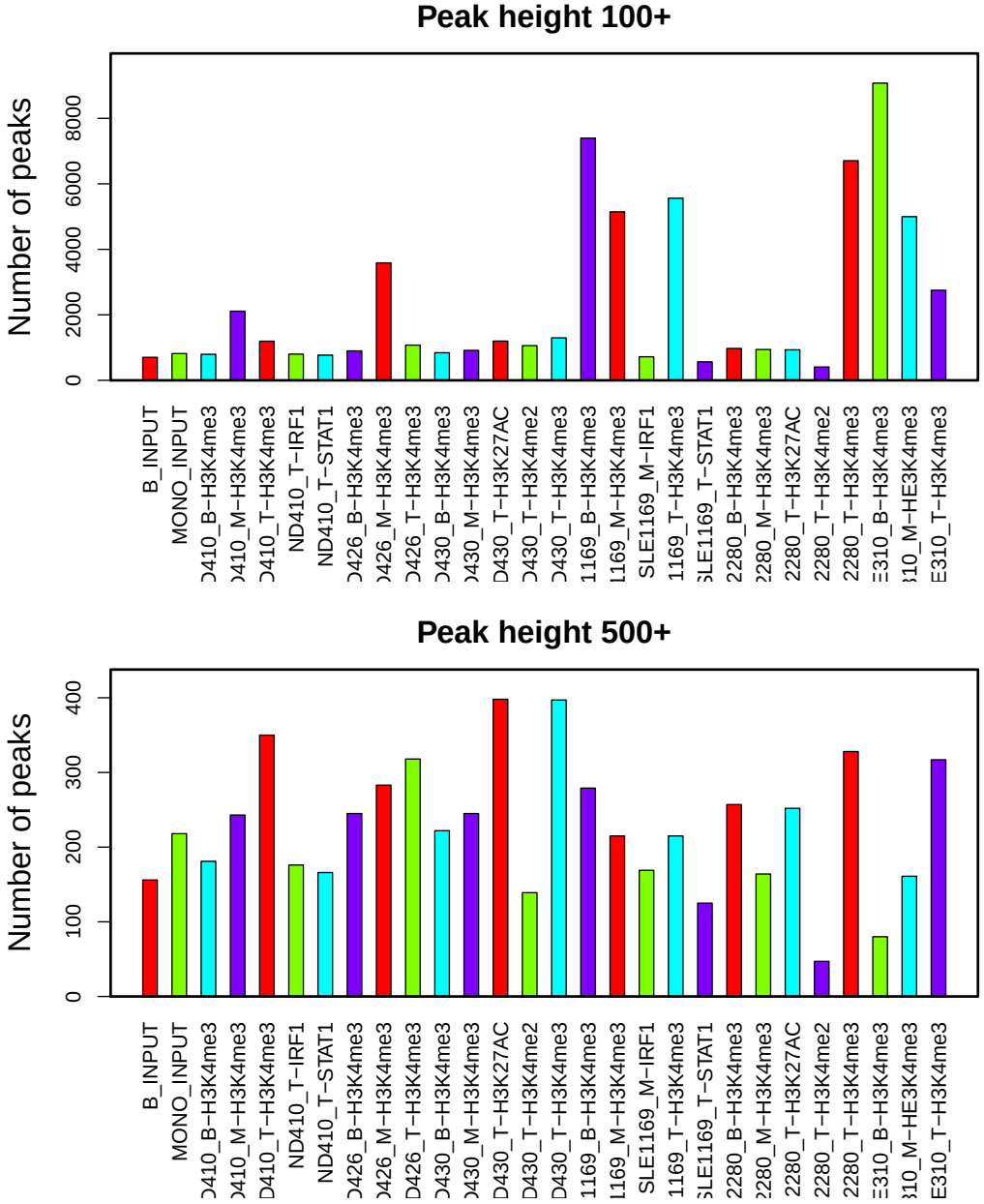
Peak height 100+
Number of peaks
0
2000
4000
6000
8000
B_INPUT
MONO_INPUT
D410_B−H3K4me3
D410_M−H3K4me3
D410_T−H3K4me3
ND410_T−IRF1
ND410_T−STAT1
D426_B−H3K4me3
D426_M−H3K4me3
D426_T−H3K4me3
D430_B−H3K4me3
D430_M−H3K4me3
D430_T−H3K27AC
D430_T−H3K4me2
D430_T−H3K4me3
1169_B−H3K4me3
1169_M−H3K4me3
SLE1169_M−IRF1
1169_T−H3K4me3
SLE1169_T−STAT1
2280_B−H3K4me3
2280_M−H3K4me3
2280_T−H3K27AC
2280_T−H3K4me2
2280_T−H3K4me3
E310_B−H3K4me3
310_M−HE3K4me3
E310_T−H3K4me3
Peak height 500+
Number of peaks
0
100
200
300
400
B_INPUT
MONO_INPUT
D410_B−H3K4me3
D410_M−H3K4me3
D410_T−H3K4me3
ND410_T−IRF1
ND410_T−STAT1
D426_B−H3K4me3
D426_M−H3K4me3
D426_T−H3K4me3
D430_B−H3K4me3
D430_M−H3K4me3
D430_T−H3K27AC
D430_T−H3K4me2
D430_T−H3K4me3
1169_B−H3K4me3
1169_M−H3K4me3
SLE1169_M−IRF1
1169_T−H3K4me3
SLE1169_T−STAT1
2280_B−H3K4me3
2280_M−H3K4me3
2280_T−H3K27AC
2280_T−H3K4me2
2280_T−H3K4me3
E310_B−H3K4me3
310_M−HE3K4me3
E310_T−H3K4me3

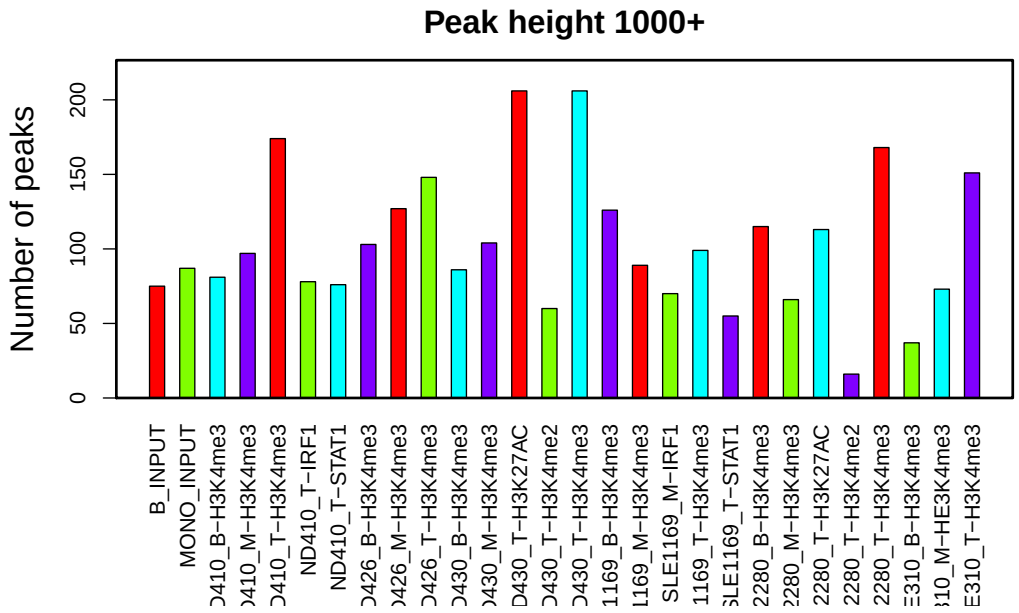

2.3 5-UTR peaks

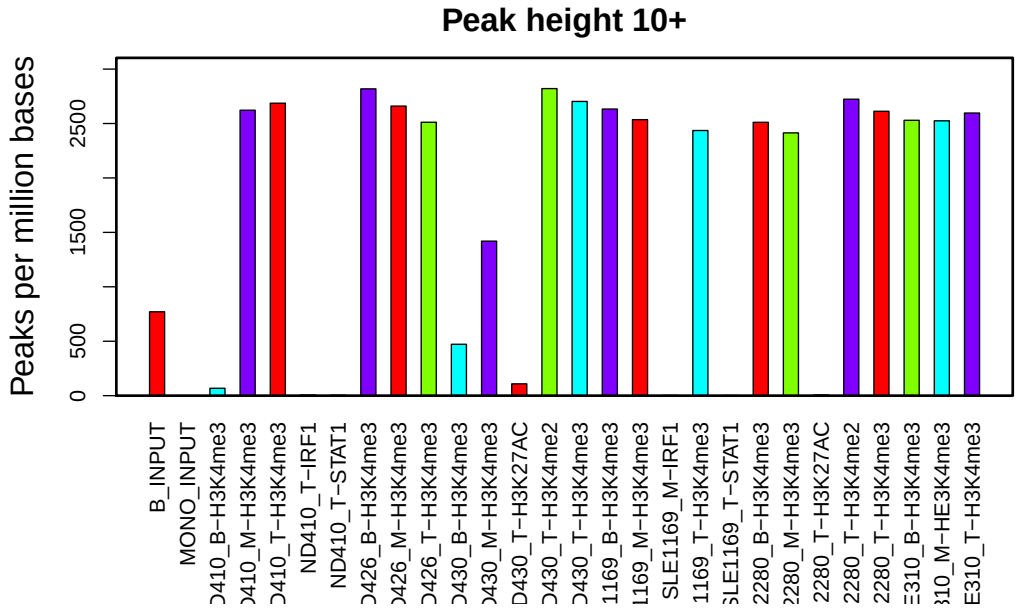

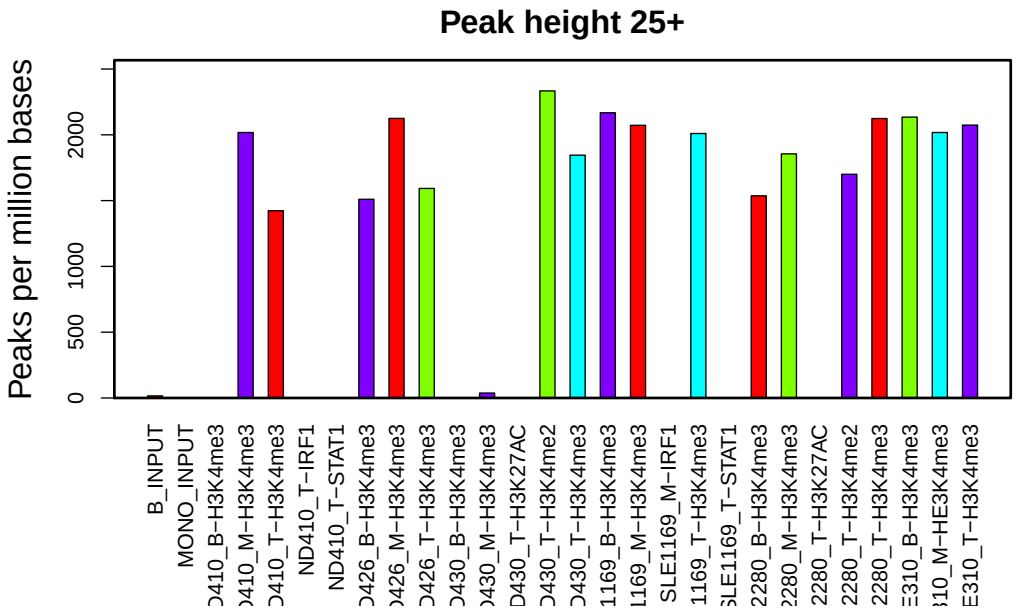
Peak height 25+
Peaks per million bases
0
500
1000
2000
B_INPUT
MONO_INPUT
D410_B−H3K4me3
D410_M−H3K4me3
D410_T−H3K4me3
ND410_T−IRF1
ND410_T−STAT1
D426_B−H3K4me3
D426_M−H3K4me3
D426_T−H3K4me3
D430_B−H3K4me3
D430_M−H3K4me3
D430_T−H3K27AC
D430_T−H3K4me2
D430_T−H3K4me3
1169_B−H3K4me3
1169_M−H3K4me3
SLE1169_M−IRF1
1169_T−H3K4me3
SLE1169_T−STAT1
2280_B−H3K4me3
2280_M−H3K4me3
2280_T−H3K27AC
2280_T−H3K4me2
2280_T−H3K4me3
E310_B−H3K4me3
310_M−HE3K4me3
E310_T−H3K4me3

2.4 TSS reads

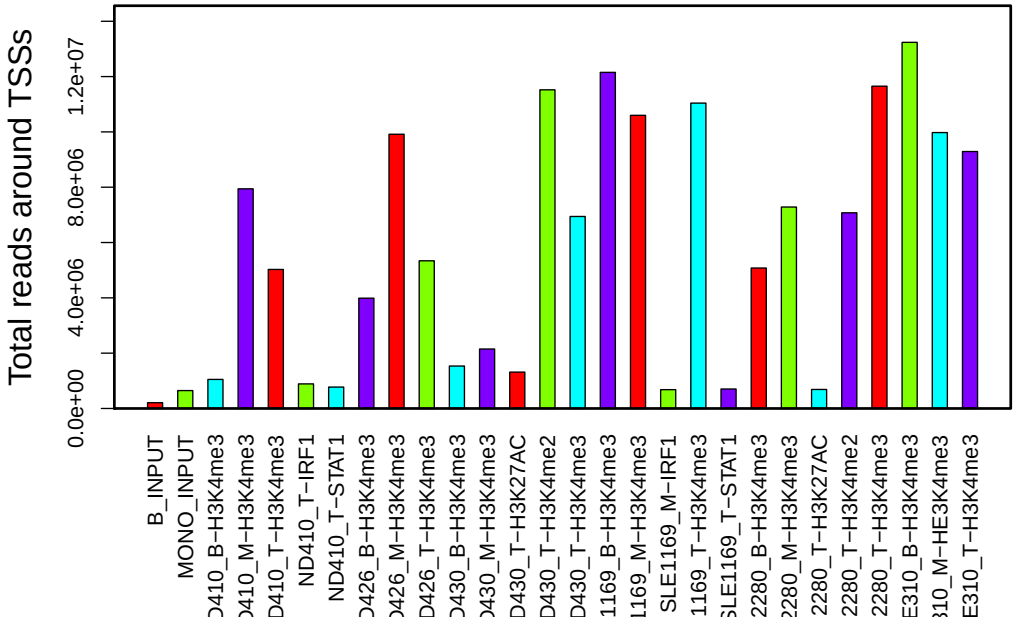
Total reads around TSSs
0.0e+00
4.0e+06
8.0e+06
1.2e+07
B_INPUT
MONO_INPUT
D410_B−H3K4me3
D410_M−H3K4me3
D410_T−H3K4me3
ND410_T−IRF1
ND410_T−STAT1
D426_B−H3K4me3
D426_M−H3K4me3
D426_T−H3K4me3
D430_B−H3K4me3
D430_M−H3K4me3
D430_T−H3K27AC
D430_T−H3K4me2
D430_T−H3K4me3
1169_B−H3K4me3
1169_M−H3K4me3
SLE1169_M−IRF1
1169_T−H3K4me3
SLE1169_T−STAT1
2280_B−H3K4me3
2280_M−H3K4me3
2280_T−H3K27AC
2280_T−H3K4me2
2280_T−H3K4me3
E310_B−H3K4me3
310_M−HE3K4me3
E310_T−H3K4me3

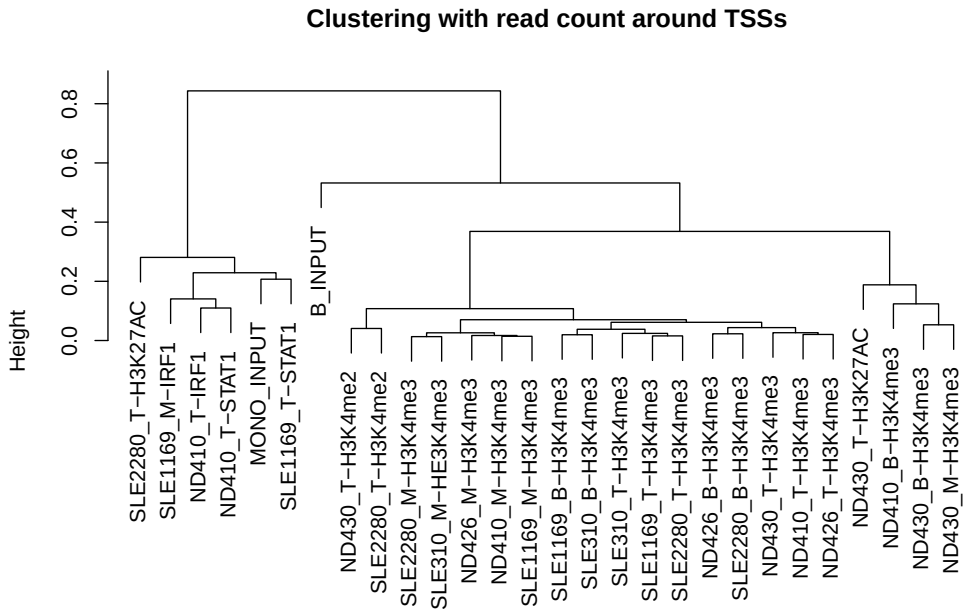
Clustering with read count around TSSs
Height
0.0
0.2
0.4
0.6
0.8
SLE2280_T−H3K27AC
SLE1169_M−IRF1
ND410_T−IRF1
ND410_T−STAT1
MONO_INPUT
SLE1169_T−STAT1
B_INPUT
ND430_T−H3K4me2
SLE2280_T−H3K4me2
SLE2280_M−H3K4me3
SLE310_M−HE3K4me3
ND426_M−H3K4me3
ND410_M−H3K4me3
SLE1169_M−H3K4me3
SLE1169_B−H3K4me3
SLE310_B−H3K4me3
SLE310_T−H3K4me3
SLE1169_T−H3K4me3
SLE2280_T−H3K4me3
ND426_B−H3K4me3
SLE2280_B−H3K4me3
ND430_T−H3K4me3
ND410_T−H3K4me3
ND426_T−H3K4me3
ND430_T−H3K27AC
ND410_B−H3K4me3
ND430_B−H3K4me3
ND430_M−H3K4me3

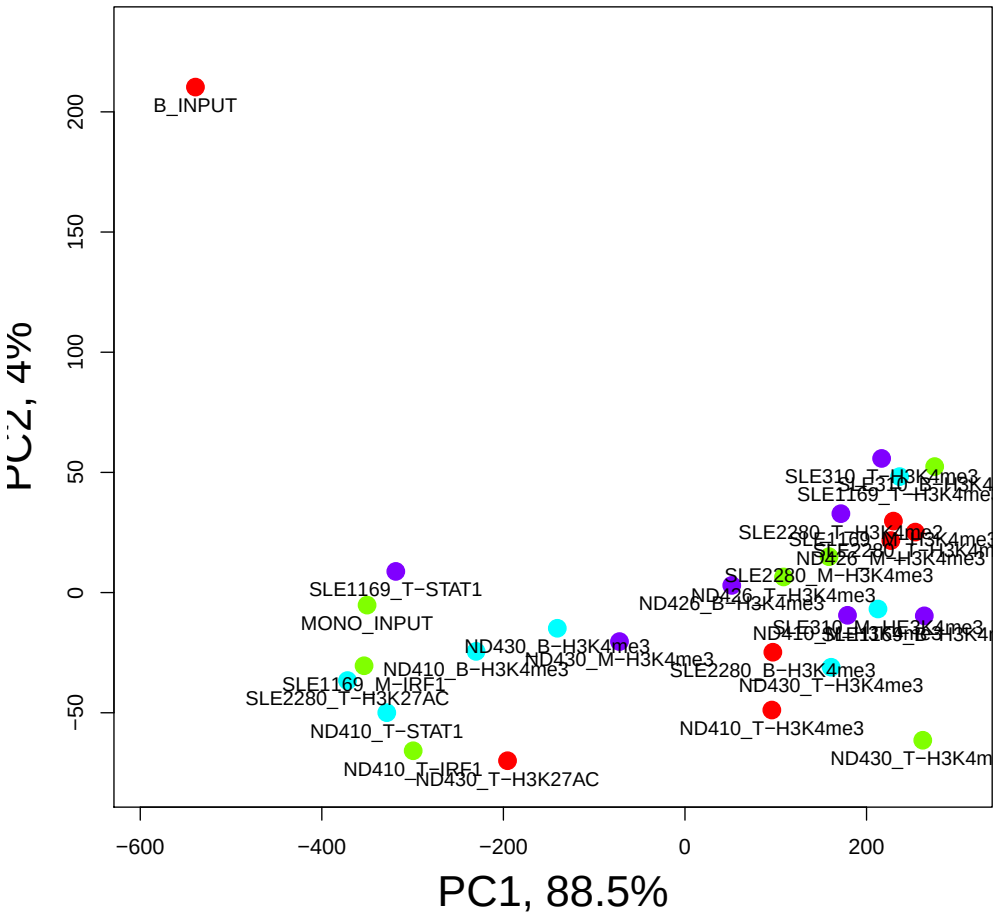
B_INPUT
SLE1169_T−STAT1
MONO_INPUT
ND430_B−H3K4me3
ND430_M−H3K4me3
ND410_B−H3K4me3
SLE1169_M−IRF1
SLE2280_T−H3K27AC
ND410_T−STAT1
ND410_T−IRF1
ND430_T−H3K27AC
SLE2280_M−H3K4me3
SLE2280_B−H3K4me3
ND430_T−H3K4me3
ND410_T−H3K4me3
ND430_T−H3K4m
PC2, 4%
PC1, 88.5%
200
150
100
50
0
−50
−600
−400
−200
0
200